Chapter 9

Gene cluster involved in lipopolysaccharide-core biosynthesis and identification of a novel lipid A modification in *Bordetella pertussis*

Jeroen Geurtsen, Monika Dzieciatkowska, Liana Steeghs, Annemarie Boleij, Kelly Broen, Hendrik-Jan Hamstra, Jianjun Li, Jim Richards, Jan Tommassen, and Peter van der Ley

Submitted for publication

Abstract

Lipopolysaccharide (LPS), also known as endotoxin, is one of the main constituents of the Gram-negative bacterial outer membrane. Whereas its lipid A part is generally seen as the main determinant for endotoxic activity, the oligosaccharide moiety plays an important role in the interaction with professional antigen-presenting cells, such as dendritic cells. Here, we describe a novel four-gene cluster involved in the biosynthesis of the *Bordetella pertussis* core oligosaccharide. By insertionally inactivating the genes and studying the resulting LPS structures, we show that at least two of the genes encode active glycosyltransferases. In addition, we demonstrate that mutations in the operon differentially affect dendritic cell maturation and macrophage activation. Interestingly, we also found a previously unknown modification of lipid A with a hexosamine.

Introduction

LPS is an amphiphilic molecule located in the outer leaflet of the outer membrane of Gram-negative bacteria. LPS possesses both endotoxic activity and adjuvant activity. Both properties are based upon its recognition by the host TLR4/MD-2 receptor complex (reviewed in Pålsson-McDermott and O'Neill, 2004; O'Neill, 2006). LPS consists of three distinct structural domains: lipid A, the core, and the O-antigen. Lipid A functions as a hydrophobic membrane anchor and forms the bioactive component of the molecule (Takada and Kotani, 1989). The core region consists of a complex oligosaccharide, which, as compared to the O-antigen, shows only limited structural variability. In some bacteria, e.g., *Enterobacteriaceae*, the core oligosaccharide (core OS) can be divided into an inner core and an outer core. The outer core primarily consists of pyranosidic hexoses, e.g., D-glucose, D-galactose, and D-glucosamine, whereas the inner core primarily consists of octulosonic acids and heptopyranoses. In the vast majority of Gram-negative bacteria, the core domain is connected to the lipid A domain by a specific carbohydrate, 2-keto-3-deoxyoctulosonic acid (Kdo) (Raetz and Whitfield, 2002). The O-antigen comprises the most variable part of the LPS and confers bacteria serotype specificity. It is composed of repeating sugar subunits of one to eight sugars. Each O-chain can contain up to 50 of these subunits. The O-antigen has been implicated in bacterial immune escape, especially the escape from serum complement-mediated lysis (Raetz and Whitfield, 2002).

In contrast to the LPS of *Bordetella bronchiseptica* and *Bordetella parapertussis*, the LPS of *Bordetella pertussis* never contains an O-antigen domain (Peppler, 1984; Di Fabio *et al.*, 1992). Therefore, *B. pertussis* LPS is often referred to as lipooligosaccharide. *B. pertussis* produces two dominant LPS forms, band A and band B LPS (Peppler, 1984). Band B LPS is composed of lipid A and a core oligosaccharide consisting of 9 carbohydrates (Caroff *et al.*, 2000). Addition of a terminal trisaccharide, consisting of *N*-acetyl glucosamine, 2,3-diacetamido-2,3-dideoxy-mannuronic acid, and 2-acetamido-4-*N*-methyl-2,4-dideoxy-fucose, to band B LPS forms the LPS referred to as band A.

In *Escherichia coli* and *Salmonella enterica* serovar Typhimurium, the core OS biosynthesis gene cluster consists of three operons, designated the *gmhD*, *waaQ*, and *WaaA* operons. The *gmhD* operon consists of four genes, *gmhD* and *waaFCL*, which are involved in the synthesis of the inner core (Schnaitman and Klena, 1993). The *gmhD*, *waaF*, and *waaC* genes encode proteins involved in the biosynthesis and transfer of Heptoses I and II to Kdo_2-lipid A (Schnaitman and Klena, 1993), whereas the *waaL* gene product is a ligase that is involved in the attachment of the O-antigen (MacLachlan *et al.*, 1991). The *waaQ* operon is the largest of the three operons and encodes proteins

that are involved in the biosynthesis of the outer core and in modification/decoration of the core OS. The number and types of genes present within in the *waaQ* operon differs per strain, which explains the strain-specific differences in core composition (Heinrichs *et al.*, 1998). The *waaA* operon often encodes only one protein, KdtA. Only in *E. coli* K-12, an additional non LPS-related open reading frame (ORF) is present (Raetz and Whitfield, 2002). The *kdtA* gene of *Enterobacteriaceae* encodes the bifunctional Kdo transferase that adds the two Kdo residues in the Kdo_2-lipid A biosynthesis (Clementz and Raetz, 1991).

Although the *Bordetella* and *E. coli* core OS show some resemblance, the exact composition and configuration of residues display marked differences. For example, the *Bordetella* core OS contains only one Kdo residue, instead of the two or three residues that are found in most other Gram-negative bacteria, including *E. coli*. Recently, this was shown to be due to the functioning of *Bordetella* KdtA as a monofunctional, rather than as a bifunctional Kdo transferase (Isobe *et al.*, 1999). Like in *E. coli*, the *Bordetella* core OS starts with two heptose residues attached to Kdo. The responsible glycosyltransferases were identified and shown, as expected, to be homologues of the WaaC and WaaF enzymes, respectively (Allen *et al.*, 1998a; Sisti *et al.*, 2002). Additionally, the *wlb* locus encompassing the genes responsible for the addition of the terminal trisaccharide in band A LPS has been identified (Allen and Maskell, 1996; Allen *et al.*, 1998b). The enzymes responsible for the synthesis of the remaining portion of the *Bordetella* core OS are currently unknown and await further identification.

Although its lipid A part is generally seen as the main determinant for the biological activity of LPS through the activation of the TLR4/MD-2 receptor complex, the oligosaccharide region can also play an important role in its interaction with antigen-presenting cells (APCs). Receptors implicated in this type of LPS recognition include the complement receptor CR3 and the scavenger receptor SR-A (van Amersfoort *et al.*, 2003; Plüddemann *et al.*, 2006). In the case of *Neisseria meningitidis*, the LPS oligosaccharide region has been shown to be a critical determinant for the bacterial interaction with dendritic cells (DCs) (Uronen-Hansson *et al.*, 2004; Kurzai *et al.*, 2005; Steeghs *et al.*, 2006). Interestingly, among a panel of mutants with a truncated LPS oligosaccharide chain, the *lgtB* mutant lacking only the terminal galactose residue of the lacto-*N*-neotetraose unit showed a strongly increased association with DCs, also resulting in higher uptake of the bacteria (Steeghs *et al.*, 2006). This interaction was shown to be entirely mediated by the C-type lectin DC-SIGN (Steeghs *et al.*, 2006). By analogy, *B. pertussis* mutants with an altered oligosaccharide chain might also be affected in their interaction with DCs. Specific targeting to APCs, such as DCs, could conceivably affect the outcome of the immune response against a whole-cell pertussis

vaccine. As a first step towards improvement of whole-cell vaccines by this route, we have now identified a gene cluster involved in LPS oligosaccharide biosynthesis in *B. pertussis*, identified the LPS alterations in the knockout mutants, and studied the effects of the mutations on interaction with DCs and endotoxic activity. Interestingly, during our analysis, we also found a previously unknown modification of lipid A.

Materials and Methods

Bacterial strains and growth conditions

All bacterial strains used are described in Table 1. Typically, the *E. coli* strains were grown at 37°C in Luria-Bertani broth while shaking at 200 rpm. When appropriate, bacteria were grown in the presence of 100 μg/ml ampicillin, 50 μg/ml kanamycin, or 10 μg/ml gentamicin, for plasmid maintenance or strain selection. *B. pertussis* was grown in synthetic THIJS medium (Thalen *et al.*, 1999) or on Bordet-Gengou (BG) agar supplemented with 15% defibrinated sheep blood (Tritium) at 35°C.

TABLE 1
Bacterial strains and plasmids

Strain or plasmid	Genotype or description	Source or reference
Strains		
B. pertussis		
B213	Streptomycin resistant derivative of *B. pertussis* strain Tohama	Kasuga et al. (1953)
B213 ΔBP2328	BP2328 mutant of strain B213, Str^R, Km^R	This study
B213 ΔBP2329	BP2329 mutant of strain B213, Str^R, Km^R	This study
B213 ΔBP2331	BP2331 mutant of strain B213, Str^R, Km^R	This study
E. coli		
TOP10F'	*F´{lacI^q Tn10 (Tet^R)} mcrA Δ(mrr-hsdRMS-mcrBC) Φ80lacZΔM15 ΔlacX74 deoR recA1 araD139 Δ (ara-leu)7697 galU galK rpsL endA1 nupG*	Invitrogen
DH5α	*F$^-$ Δ(lacZYA-algF)U169 thi-1 hsdR17 gyrA96 recA1 endA1 supE44 relA1 phoA Φ80 dlacZΔM15*	Hanahan (1983)
SM10(λpir)	*thi thr leu fhyA lacY supE recA*::RP4-2-Tc::Mu λ *pir* R6K Km^R	N.V.I.[a]
Plasmids		
pGEM-T Easy	*E. coli* cloning vector Amp^R	Promega
pUC4K	*E. coli* vector harbouring kanamycin-resistance cassette, Amp^R Km^R	Viera and Messing, 1982
pSS1129	Allelic exchange vector, *bla gen rpsL oriVColE1 oriT λ cos*	Stibitz, 1994
pGEM-BP2328$_{up}$	pGEM-T Easy derivative harbouring BP2328 upstream sequence	This study
pGEM-BP2328$_{down}$	pGEM-T Easy derivative harbouring BP2328 downstream sequence	This study
pGEM-BP2329$_{up}$	pGEM-T Easy derivative harbouring BP2329 upstream sequence	This study
pGEM-BP2329$_{down}$	pGEM-T Easy derivative harbouring BP2329 downstream sequence	This study
pGEM-BP2331	pGEM-T Easy derivative harbouring BP2331 sequence	This study
pSS1129-BP2328$_{KO}$	pSS1129 derivative harbouring BP2328 knock out construct, Km^R	This study
pSS1129-BP2329$_{KO}$	pSS1129 derivative harbouring BP2329 knock out construct, Km^R	This study
pSS1129-BP2331$_{KO}$	pSS1129 derivative harbouring BP2331 knock out construct, Km^R	This study

[a] Netherlands Vaccine Institute, Bilthoven, The Netherlands

Recombinant DNA techniques

All plasmids used are described in Table 1. Plasmid DNA was isolated using the Promega Wizard®*Plus* SV Minipreps system. Restriction endonucleases were used according to the instructions of the manufacturer (Roche). DNA fragments were isolated from agarose gels using the Promega Wizard® SV Gel and PCR Clean-Up system. Ligations were performed using the rapid DNA ligation kit (Roche).

All primers used are described in Table 2. Chromosomal template DNA for PCR reactions was prepared by resuspending ~10^9 bacteria in 50 μl of distilled water, after which the suspension was heated for 15 min at 95°C. The suspension was then centrifuged for 1 min at 16,100 x *g*, after which the supernatant was used as template DNA. To construct *B. pertussis* mutant strains B213ΔBP2328 and ΔBP2329, we amplified DNA segments encompassing the 5' region and upstream sequences of the corresponding ORFs by using primers BP2328_FW_{up}, BP2329_FW_{up}, and primers BP2328_REV_{up} and BP2329_REV_{up}, which both contained a BamHI site. Additionally, DNA fragments containing the 3' regions and downstream sequences of the ORFs were obtained by PCR with primers BP2328_FW_{down}, BP2329_FW_{down}, both containing a BamHI site, and primers BP2328_REV_{down} and BP2329_REV_{down}. To construct a *B. pertussis* BP2331 mutant strain, the corresponding ORF was amplified by using primers BP2331_FW and BP2331_REV. The PCRs were performed using pure Taq Ready-to-go PCR beads (Amersham Biosciences) in a 25-μl total reaction volume with 5 pmol of each primer. The temperature program was as follows: 95°C for 3 min, 30 cycles of 15 s at 95°C, 30 s at 55°C, and 1 min at 72°C, followed by 7 min at 72°C and subsequent cooling to 4°C. The PCR products were purified from agarose gel and subsequently cloned into pGEM-T Easy resulting in plasmids pGEM-BP2328$_{up}$, pGEM-BP2328$_{down}$, pGEM-BP2329$_{up}$, pGEM-BP2329$_{down}$, and pGEM-BP2331, respectively. The BamHI–SpeI

TABLE 2

Primers

Name	Sequence (5'-3')[a]
BP2328_FW_{up}	TTCCGCACTTACTGGCTGAG
BP2328_FW_{down}	GGATCCTCGCGGTACGACAGCACAT
BP2328_REV_{up}	GGATCCTGTTGCGCGAGATGCTGGAG
BP2328_REV_{down}	CCTCATCGCCAAGGTCAATC
BP2329_FW_{up}	TCACCTTCGACGACGGATAC
BP2329_FW_{down}	GGATCCGTGCGCATCTACCTGATCC
BP2329_REV_{up}	GGATCCGAATCGACCACGATGAAC
BP2329_REV_{down}	GATCCAGCTTGGCCTGGTTG
BP2331_FW	GTGACGTGGTGGTACATCAG
BP2331_REV	TGGTCTACCGCAGGAACAAT

[a] BamHI restriction sites are underlined

fragments of pGEM-BP2328$_{down}$ and pGEM-BP2329$_{down}$ were ligated into *Bam*HI–*Spe*I-restricted pGEM-BP2328$_{up}$ and pGEM-BP2329$_{up}$, respectively. The resulting plasmids and plasmid pGEM-BP2331 were cut with BamHI and EcoRV, respectively, to allow for insertion of the kanamycin-resistance cassette from plasmid pUC4K obtained by BamHI and HinDII digestion, respectively. Finally, EcoRI fragments of the constructs obtained were ligated into the EcoRI-restricted suicide plasmid pSS1129. The final constructs, designated pSS1129-BP2328$_{KO}$, pSS1129-BP2329$_{KO}$, and pSS1129-BP2331$_{KO}$, respectively, contained the kanamycin-resistance cassette in the same orientation as the transcription direction of the operon. The pSS1129-based plasmids were used to transform *E. coli* SM10(λpir), which allowed for subsequent transfer of the plasmids to *B. pertussis* and construction of *B. pertussis* BP2328, BP2329, and BP2331 mutants by allelic exchange. Transformants were screened by PCR using various primer sets.

LPS isolation and preparation of de-*O*-acylated LPS

LPS was isolated using the hot phenol/water extraction method (Westphal and Jann, 1965) with slight modifications (Geurtsen *et al.*, 2006). De-*O*-acylation of LPS was achieved by mild hydrazinolysis (Holst, 2000). Briefly, LPS was dissolved in anhydrous hydrazine (200 μl), and incubated at 37°C for 50 min with constant stirring to release the *O*-linked fatty acyl chains. The mixture was cooled and 600 μl of cold acetone were added in small portions to convert hydrazine to acetone hydrazone. The precipitate of the de-*O*-acylated LPS was collected by centrifugation (4000 x *g*, at 7°C for 30 min). The pellet was washed twice with 600 μl of cold acetone, centrifuged and dissolved in water before lyophilisation.

Capillary electrophoresis-electrospray mass spectrometry

A Prince CE system (Prince Technologies) was coupled to a 4000 QTRAP mass spectrometer (Applied Biosystems/MDS Sciex). A sheath solution (isopropanol-methanol, 2:1) was delivered at a flow rate of 1.0 μl/min. Separations were obtained on a ~90-cm length bare fused-silica capillary using 15 mM ammonium acetate in deionised water, pH 9.0. The 5 kV and –5 kV of electrospray ionisation voltage were used for positive and negative ion mode detections, respectively. For all the mass spectrometric experiments, nitrogen was used as curtain and collision gas. In the MS^2 (enhanced product ion scan or EPI) and MS^3 experiments, the scan speed was set to 4000 Da/s with Q_0 trapping, the trap fill time was set as “dynamic” and the resolution of Q1 was set as “unit”. For MS^3 experiments, the excitation coefficient was set at a value to excite only the first isotope for a single charged precursor with excitation time set at 100 ms.

LPS analysis by Tricine-SDS-PAGE

Approximately 10^9 bacteria were suspended in 50 μl of sample buffer (Laemmli, 1970), and 0.5 mg/ml proteinase K (end concentration) was added. The samples were incubated for 60 min at 55°C, followed by 10 min at 95°C to inactivate proteinase K. The samples were then diluted 10 fold by adding sample buffer, after which 2 μl of each sample were applied to a Tricine-SDS-PAGE gel (Lesse *et al.*, 1990). The bromophenol blue was allowed to run into the separating gel at 35 V, after which the voltage was increased to 105 V. After the front reached the bottom of the gel, electrophoresis was continued for another 45 min. The gels were fixed overnight in water/ethanol/acetic acid 11:8:1 (v/v/v) and subsequently stained with silver as described (Tsai and Frasch, 1982).

Preparation of bacterial cell suspensions

Bacteria were inactivated in 0.5% paraformaldehyde (PFA) in phosphate-buffered saline (PBS) for 30 min and washed thoroughly in RPMI 1640 medium without phenol red (Gibco). Bacterial suspensions with an optical density at 600 nm (A600) of 1, corresponding to ~10^9 bacteria/ml, were prepared in RPMI 1640 medium without phenol red.

Human DC generation and culture

Immature human DC were generated from human peripheral blood mononuclear cells (PBMCs) as described previously with minor modifications (Sallusto and Lanzavecchia, 1994). Briefly, PBMCs were isolated from heparinised blood from healthy volunteers using density-gradient centrifugation over a Ficoll gradient (Amersham Biosciences). Recovered PBMC fractions were washed three times in RPMI 1640 medium, supplemented with 10% heat-inactivated fetal calf serum (FCS) (Bodinco BV). Next, monocytes were prepared from PBMCs by centrifugation over a three-layer Percoll gradient (GE Healthcare Bio-Sciences AB) (60%, 47.5%, and 34% Percoll in RPMI 1640, 10% FCS). Monocytes were harvested from the upper interface and washed three times with RPMI 1640, 10% FCS medium and incubated in a six-well plate (4 ml per well, 0.5x10^6 cells/ml) in RPMI 1640, 10% FCS, supplemented with 2.4 mM L-glutamine (Sigma-Aldrich), 100 U/ml penicillin-streptomycin (Gibco), 100 ng/ml of human recombinant GM-CSF (Peprotech), and 50 ng/ml of human recombinant IL-4 (Strathmann-Biotec AG). After six days of culture, immature DC (imDC) were harvested, which were negative for CD14 and CD83, expressed low levels of CD86 and HLA-DR, and expressed high levels of CD40 and CD11c as assessed by flow cytometry.

DC stimulation

ImDC were washed and resuspended at a concentration of $5x10^5$ cells/ml in RPMI 1640 10% FCS, and co-incubated with either PFA-fixed *B. pertussis* cells at a multiplicity of infection (MOI) of 10 or 100, or purified LPS at a concentration of 10 or 1000 ng/ml. Unstimulated imDC served as control in all experiments. DC were harvested after 24 h and directly stained for expression of cell surface markers; the supernatants were stored at -80°C before cytokine measurements.

Flow cytometric analysis of cell surface markers

Surface expression of DC maturation markers and co-stimulatory molecules was assessed by flow cytometry. Immature or stimulated DC were harvested, washed in RPMI 1640, 10% FCS and resuspended in filter-sterilised PBS containing 0.1% bovine serum albumin (FACS buffer). Next, cells were incubated for 30 min at 4°C with either one of the following antibodies: FITC-conjugated anti-human CD11c (mIgG1) and CD83 (mIgG1), phycoerythrin-conjugated anti-human CD86 (mIgG1) and CD40 (mIgG1), allophycocyanin-conjugated anti-human CD14 (mIgG1) and HLA-DR (mIgG2b) and appropriate fluorochrome-labelled isotype controls (CD11c, CD40 and CD14 from eBioscience; CD83, CD86 and HLA-DR from BD Pharmingen). Cells were washed twice with FACS buffer and analysed using flow cytometry (FACScan, Becton Dickinson).

Cytokine measurements

Human IL-10 and IL-12p70 concentrations in the supernatants of stimulated DCs were determined using an Enzyme-linked Immunosorbent Assay (ELISA) according to the manufacturer's instructions (BD Biosciences Pharmingen).

Endotoxic activity assays

The human macrophage cell line MM6 (Ziegler-Heitbrock *et al.*, 1988) was stimulated with serial dilutions of whole bacterial cell suspensions or purified LPS as described (Geurtsen *et al.*, 2006). The bacterial cell suspensions were prepared by collecting the cells from cultures by centrifugation, after which they were resuspended in PBS at an OD_{590} of 1.0, heat-inactivated for 10 min in the presence of 8 mM formaldehyde, and stored at 4°C. Following stimulation, IL-6 concentrations in the culture supernatants were quantified with an ELISA against human IL-6 according to the manufacturer's instructions (PeliKine Compact™).

Results

Identification of a novel LPS-biosynthesis operon in *B. pertussis*

As a glucose (β1-4) heptose linkage is a common feature of the LPS inner core in many bacteria including *B. pertussis*, we used genes encoding glycosyltransferases with this specificity from *N. meningitidis* (*lgtF/icsB*), among others, to identify homologous sequences in the *B. pertussis* Tohama genome sequence. In this way we found a cluster of four genes (BP2328 to BP2331, GenBank Accession Numbers NP_880966 to NP_880969), three of which showed high sequence similarity to LPS glycosyltransferases from various bacteria, i.e., BP2328, BP2329 and BP2331. BP2330 shows the highest similarity to a polysaccharide deacetylase from *Xylella fastidiosa*. The four ORFs are close to each other and in some cases even overlap, suggesting that they constitute an operon (Fig. 1A). The genes upstream and, in the reverse orientation, downstream of the operon, putatively encode homologues of the DNA polymerase III subunit alpha DnaE and of the putative sulfatase YhbX of *E. coli*, respectively. In order to study the role of the putative LPS glycosyltransferases, we made constructs in suicide plasmid pSS1129 carrying the individual BP2328, BP2329, and BP2331 genes interrupted by a kanamycin-resistance cassette for insertional inactivation by allelic exchange. Using

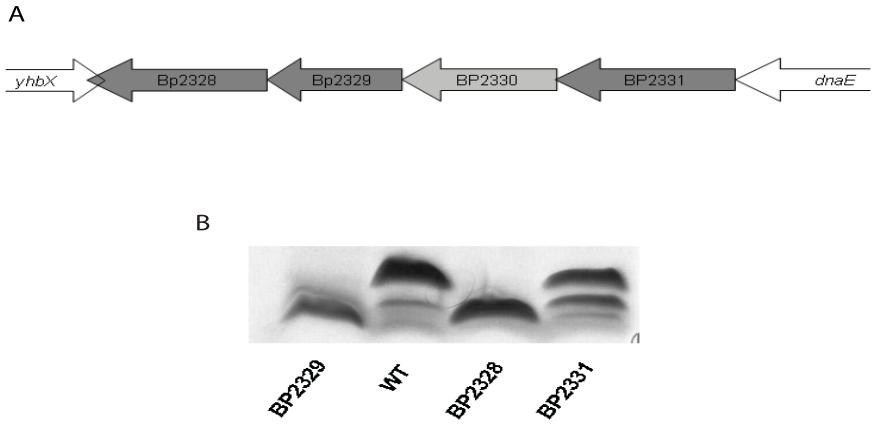

Fig. 1. (A) Schematic representation of the identified glycosyltransferase operon. Dark gray arrows indicate the genes that encode putative glycosyltransferases, whereas the light grey and white arrows indicate the gene encoding a putative monosaccharide deacetylase and the flanking ORFs, respectively. (B) Analysis of LPS profiles from the wild-type *B. pertussis* strain (WT), and the BP2329-, BP2328-, and BP2331-mutant strains by Tricine-SDS-PAGE.

this approach, knockout mutants for all three genes could be readily obtained in *B. pertussis* strain B213. Analysis of their LPS by Tricine-SDS-PAGE of whole-cell lysates showed clearly truncated LPS for the BP2328 and BP2329 mutants (Fig. 1B). In contrast, the LPS of the BP2331 mutant strain was more heterogenic and consisted of multiple bands, including the wild-type length.

LPS structural analysis

To determine their structure, LPS from the wild-type and BP2328-, BP2329-, and BP2331-mutant strains was isolated, *O*-deacylated, and analysed by ESI-MS in the negative-ion mode (Fig. 2). The proposed LPS compositions are summarised in Table 3. The spectrum of wild-type LPS (Fig. 2A) revealed a major triply-charged ion at *m/z* 1108.5 corresponding to full-length *B. pertussis* LPS with the composition GlcNAc•Man2NAc3NAcA•Fuc2NAc4NMe•GalNA•Glc•$GlcN_2$•GlcA•Hep_3•*P*•Kdo•lipid A-OH. Additional ions were present at *m/z* 770.1 ($[M-3H]^{3-}$), 811.1 ($[M-4H]^{4-}$), 831.4 ($[M-4H]^{4-}$), 888.3 ($[M-3H]^{3-}$), 951.8 ($[M-H]^{-}$), 987.1 ($[M-2H]^{2-}$), 1081.7 ($[M-3H]^{3-}$), 1121.1 ($[M-3H+K]^{3-}$), 1155.0 ($[M-2H]^{2-}$), and 1162.1 ($[M-3H]^{3-}$). Most of these ions corresponded to dephosphorylated or truncated glycoforms; however, the triply-charged ion at *m/z* 1162.1 corresponded to full-length *B. pertussis* LPS substituted with an additional hexosamine moiety (Table 3).

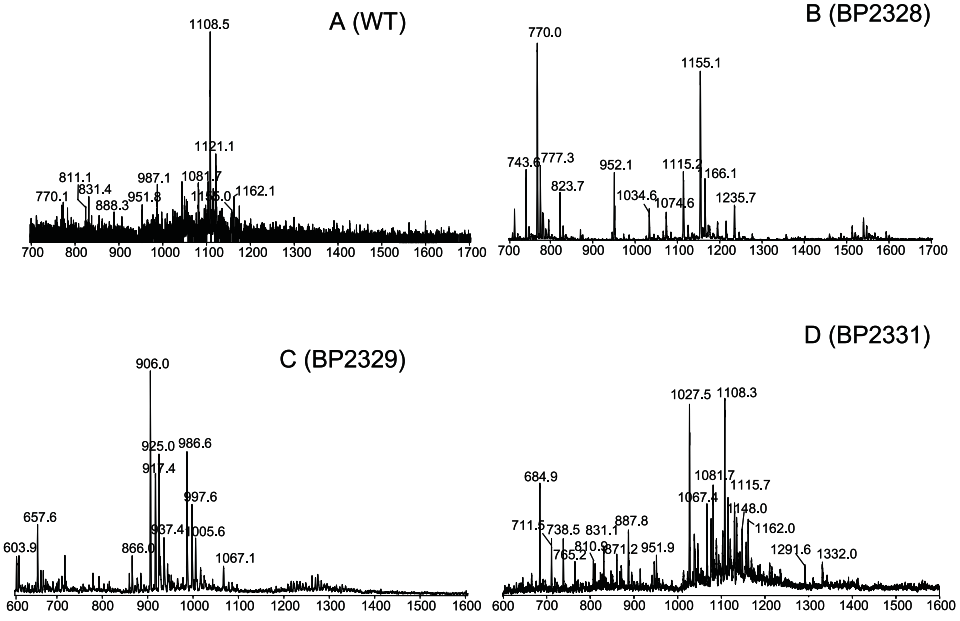

Fig. 2. Negative ion ESI-MS of *O*-deacylated LPS of wild-type *B. pertussis* (A) and *B. pertussis* mutant strains BP2328 (B), BP2329 (C) and BP2331 (D).

TABLE 3

Negative ion ESI-MS data and proposed compositions for *O*-deacylated LPS of wild-type *B. pertussis* and *B. pertussis* mutant strains BP2331, BP2328, and BP2329. Average mass units were used for calculation of molecular mass values based on proposed compositions as follows: glucose (Glc), 162.14; heptose (Hep), 192.17; 2-keto-3-deoxyoctulosonic acid (Kdo), 220.18; phosphate (*P*), 79.98; glucosamine (GlcN),161.17; hexosamine (HexN), 161.17; glucuronic acid (GlcA), 176.13; *N*-acetyl-glucosamine (GlcNAc), 203.19; 2-acetamido-4-*N*-methyl-2,4-dideoxy-fucose (Fuc2NAc4NMe), 200.12; 2,3-acetamido-2,3-dideoxy-mannuronic acid (Man2NAc3NAcA), 258.09; galactosaminuronic acid (GalNA),175.13 and lipid A-OH, 953.02. Table does not include sodium and potassium adducts and singly-charged lipid A-OH ions (*m/z* 952 ($[M-H]^-$)).

Sample	*Observed ions [m/z]*			*Molecular mass [Da]*		*Relative amount*	*Proposed composition*
	$[M-4H]^{4-}$	$[M-3H]^{3-}$	$[M-2H]^{2-}$	Observed	Calculated		
WT			987.1	1976.2	1975.8	0.30	Glc•GlcA•Hep_2•*P*•Kdo•lipid A-OH
		770.1	1155.0	2312.7	2312.1	0.20	GalNA•Glc•GlcN•GlcA•Hep_2•*P*•Kdo•lipid A-OH
		888.3		2667.9	2665.4	0.18	GalNA•Glc•$GlcN_2$•GlcA•Hep_3•*P*•Kdo•lipid A-OH
	811.1	1081.7		3248.3	3246.9	0.42	GlcNAc•Man2NAc3NAcA•Fuc2NAc4NMe•GalNA•Glc•$GlcN_2$•GlcA•Hep_3•Kdo•lipid A-OH
	831.4	1108.5		3329.0	3326.8	1.0	GlcNAc•Man2NAc3NAcA•Fuc2NAc4NMe•GalNA•Glc•$GlcN_2$•GlcA•Hep_3•*P*•Kdo•lipid A-OH
		1162.1		3489.3	3488.0	0.32	HexN•GlcNAc•Man2NAc3NAcA•Fuc2NAc4NMe•GalNA•Glc•$GlcN_2$•GlcA•Hep_3•*P*•Kdo•lipid A-OH
BP2328		743.6	1115.2	2233.1	2232.1	0.29	GalNA•Glc•GlcN•GlcA•Hep_2•Kdo•lipid A-OH
		770.0	1155.1	2312.6	2312.1	1.0	GalNA•Glc•GlcN•GlcA•Hep_2•*P*•Kdo•lipid A-OH
		823.7	1235.7	2473.8	2473.3	0.24	GalNA•Glc•$GlcN_2$•GlcA•Hep_2•*P*•Kdo•lipid A-OH
			1034.6	2071.2	2070.8	0.06	GalNA•Glc•GlcA•Hep_2•Kdo•lipid A-OH
			1074.6	2151.2	2150.8	0.05	GalNA•Glc•GlcA•Hep_2•*P*•Kdo•lipid A-OH
BP2329			866.0	1734.0	1733.7	0.3	GlcA•Hep_2•Kdo•lipid A-OH
		603.9	906.0	1814.4	1813.6	1.0	GlcA•Hep_2•*P*•Kdo•lipid A-OH
			937.4	1876.8	1876.8	0.35	GlcN•GlcA•Hep_2•*P*•Kdo•lipid A-OH –H_2O
		657.6	986.6	1975.5	1974.8	0.82	GlcN•GlcA•Hep_2•*P*•Kdo•lipid A-OH
			1067.1	2136.2	2136.0	0.24	$GlcN_2$•GlcA•Hep_2•*P*•Kdo•lipid A-OH
BP2331		684.9	1027.5	2057.4	2057.0	0.82	Glc•GlcN•GlcA•Hep_2•Kdo•lipid A-OH
		711.5	1067.4	2137.2	2137.0	0.36	Glc•GlcN•GlcA•Hep_2•*P*•Kdo•lipid A-OH
		738.5		2218.5	2218.2	0.11	Glc•$GlcN_2$•GlcA•Hep_2•Kdo•lipid A-OH
		765.2	1148.0	2298.3	2298.1	0.25	Glc•$GlcN_2$•GlcA•Hep_2•*P*•Kdo• lipid A-OH
			1115.7	2233.4	2232.1	0.45	GalNA•Glc•GlcN•GlcA•Hep_2•Kdo•lipid A-OH
			1291.6	2585.2	2585.5	0.21	GalNA•Glc•$GlcN_2$•GlcA•Hep_3•Kdo•lipid A-OH
		887.8	1332.0	2666.2	2665.4	0.34	GalNA•Glc•$GlcN_2$•GlcA•Hep_3•*P*•Kdo•lipid A-OH
	810.9	1081.7		3247.9	3246.9	0.58	GlcNAc•Man2NAc3NAcA•Fuc2NAc4NMe•GalNA•Glc•$GlcN_2$•GlcA•Hep_3•Kdo•lipid A-OH
	831.1	1108.3		3328.2	3326.8	1.0	GlcNAc•Man2NAc3NAcA•Fuc2NAc4NMe•GalNA•Glc•$GlcN_2$•GlcA•Hep_3•*P*•Kdo•lipid A-OH
	871.2	1162.0		3488.9	3488.0	0.44	HexN•GlcNAc•Man2NAc3NAcA•Fuc2NAc4NMe•GalNA•Glc•$GlcN_2$•GlcA•Hep_3•*P*•Kdo•lipid A-OH

The ESI-MS spectrum of the BP2328-mutant LPS (Fig. 2B) showed triply-charged ions at *m/z* 743.6, 770.0, and 823.7, together with their corresponding doubly-charged ions at *m/z* 1115.2, 1155.1, and 1235.7. Additional peaks were present at *m/z* 777.3 ([M-3H+Na]$^{3-}$), 952.1 ([M-H]$^{-}$), 1034.6 ([M-2H]$^{2-}$), 1074.6 ([M-2H]$^{2-}$), and 1166.1 ([M-2H+Na]$^{2-}$). Assignment of the peaks revealed that the most complete core OS structure was represented by the ions at *m/z* 823.7 and 1235.7 corresponding to the composition GalNA•Glc•$GlcN_2$•GlcA•Hep_2•*P*•Kdo•lipid A-OH. BP2329 mutant LPS (Fig. 2C) showed triply charged ions at *m/z* 603.9 and 657.6, together with their corresponding doubly-charged ions at *m/z* 906.0 and 986.6. In addition, sodium and potassium adducts of these ions were present at *m/z* 917.4 and 997.6, and *m/z* 925.0 and 1005.6, respectively. Additional peaks were present at *m/z* 866.0 ([M-2H]$^{2-}$), 937.4 ([M-2H-H_2O]$^{2-}$), and 1067.1 ([M-2H]$^{2-}$). In this case, the most complete core structure was represented by the doubly-charged ion at *m/z* 1067.1 corresponding to the composition $GlcN_2$•Glc A•Hep_2•*P*•Kdo•lipid A-OH. BP2331 mutant LPS (Fig. 2D) showed a large number of peaks, including triply-charged ions at *m/z* 1108.3 and 1162.0 corresponding to full-length *B. pertussis* LPS and full-length *B. pertussis* LPS substituted with an additional hexosamine, respectively.

To resolve the location of the additional hexosamine moiety, which was observed in both wild-type and BP2331-mutant LPS, ESI-MS^2 studies were performed in negative-ion mode (Fig. 3). MS/MS spectra of the ions at *m/z* 1108.3 (Fig. 3A) and 1162.0 (Fig. 3B) both showed a singly charged fragment ion at *m/z* 951.5, which revealed that lipid A-OH, resulting from the cleavage between the Kdo-lipid A bond under collision-induced dissociation, consisted of a β-(1→6)-linked disaccharide of *N*-acylated (3OH C14) glucosamine residues, each residue being substituted with a phosphate group. The spectrum of ion at *m/z* 1162.0 also showed an additional ion at *m/z* 1112.6, which indicates that the extra hexosamine residue was directly attached to lipid A. MS^3 on *m/z* 1112.6 further supported this conclusion (Fig. 3C).

Dendritic cell activation by *B. pertussis* LPS mutants

To determine the influence of the LPS mutations on DC activation, immature DCs were co-cultured with PFA-fixed *B. pertussis* wild-type and mutant bacteria at an MOI of 10 and 100. DC activation was monitored by analysis of maturation marker (CD83 and HLA-DR) and co-stimulatory molecule (CD86 and CD40) expression by flow cytometry (Fig. 4A) and IL-10 and IL12p70 induction by ELISA (Fig. 4B). Wild-type and all mutant bacteria induced CD83, HLA-DR, CD86, and CD40 expression, demonstrating that all strains were capable of activating DCs. However, the BP2329- and BP2331-mutant bacteria were clearly less and more stimulatory, respectively, than

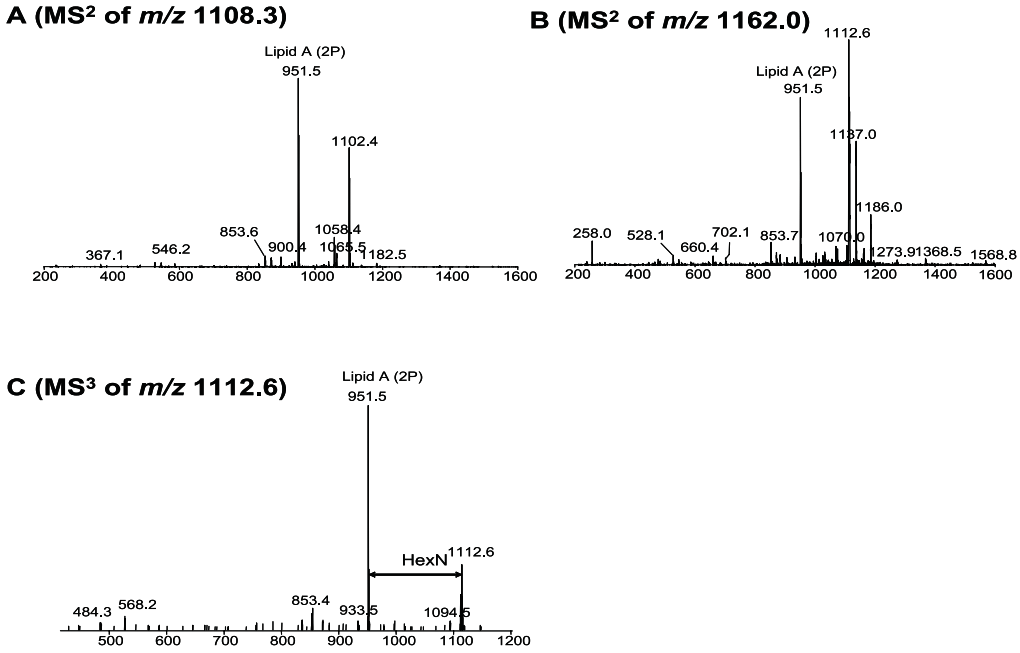

Fig. 3. Negative mode tandem mass spectrometric analysis of *O*-deacylated LPS from the BP2331-mutant strain. (A) extracted MS/MS spectrum of the ion at *m/z* 1108.3, (B) extracted MS/MS spectrum of the ion at *m/z* 1162.0, (C) extracted MS^3 spectrum of the ion at *m/z* 1112.6 from the ion at *m/z* 1162.0.

the wild-type bacteria, whereas the BP2328-mutant strain was as efficient as the wild type. The lower DC maturation observed in the case of the BP2329-mutant strain was accompanied by lower induction of IL-10 and IL-12p70 (Fig. 4B). Similarly, the BP2331 mutant, which displayed an enhanced DC-maturation capacity, induced higher amounts of IL-10 and IL-12p70. The wild-type strain and the BP2328-mutant strain induced comparable levels of IL-10, which is in agreement with the equal expression of co-stimulatory molecules and maturation markers on the DCs in response to these strains. However, whereas the wild-type strain clearly induced IL-12p70 production, this was hardly the case for the BP2328-mutant strain (Fig. 4B), suggesting that IL-10 and IL-12p70 expression can be differentially regulated.

To assess whether the observed differences in DC activation capacity between the wild-type and mutant strains are directly related to the differences in the LPS composition, DC activation studies were performed with 10 and 1000 ng/ml of purified LPS. In contrast to the high increase in expression of maturation markers and co-stimulatory molecules on DCs in response to wild-type, BP2328-, and BP2331-mutant bacteria, only minor increases in CD83, CD86, and CD40 expression (Fig. 5A) and no

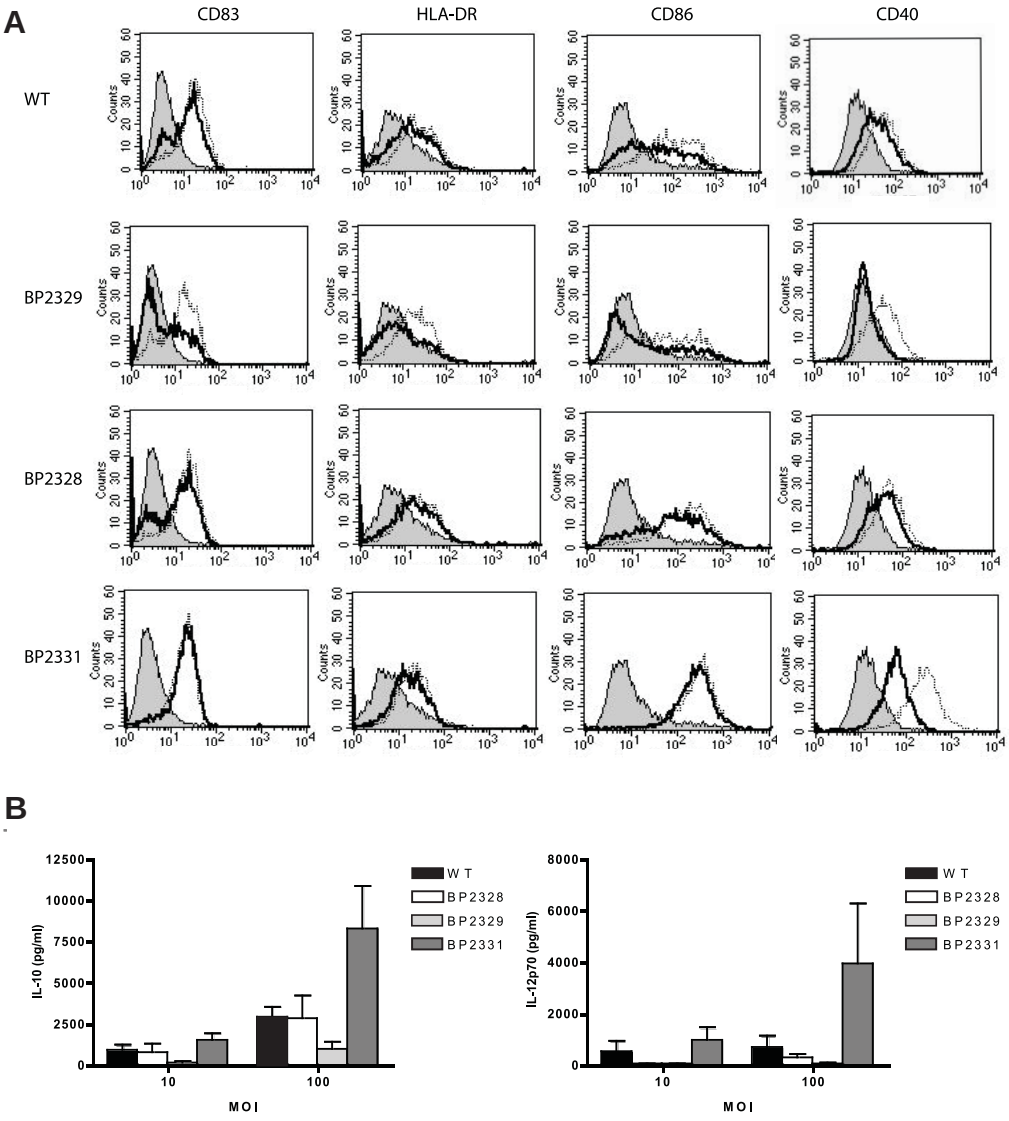

Fig. 4. DC activation after stimulation with the wild-type and mutant *B. pertussis* cells. (A) Analysis of CD83, HLA-DR, CD86, and CD40 cell-surface expression in human DCs after 24 h stimulation with PFA-fixed wild-type and mutant *B. pertussis* cells at MOI 10 (black line) or 100 (dashed line). Unstimulated DCs served as control (grey-filled histogram). Shown are FACS histograms for the indicated *B. pertussis* strains from 5,000 events counted. The vertical axis represents the cell number, while the horizontal axis represents the intensity of staining. (B) IL-10 and IL-12p70 production by cultured human DCs after stimulation with PFA-fixed wild-type and mutant *B. pertussis* cells at MOI 10 or 100. Results are expressed as mean cytokine concentrations (± SD).

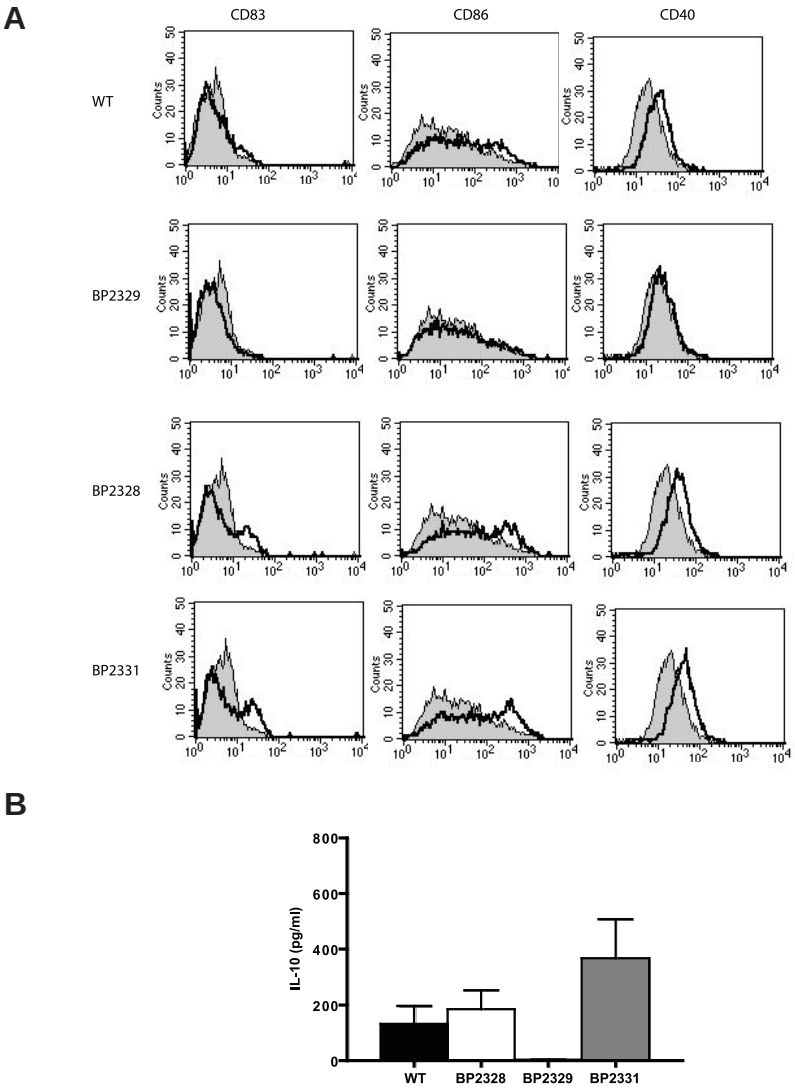

Fig. 5. DC activation after stimulation with purified wild-type and mutant *B. pertussis* LPS. (A) Analysis of CD83, CD86, and CD40 cell-surface expression in human DCs after 24 h stimulation with 1 μg/ml purified LPS. Unstimulated DCs served as control (grey-filled histogram). Shown are FACS histograms for the LPS of the indicated *B. pertussis* strains from 5,000 events counted. The vertical axis represents the cell number, while the horizontal axis represents the intensity of staining. (B) IL-10 production by cultured human DCs after stimulation with 1 μg/ml purified LPS. Results are expressed as mean cytokine concentrations (± SD).

increase in HLA-DR expression (data not shown) was found even with 1000 ng/ml LPS of these strains. Similarly, IL-10 induction was low (Fig. 5B) and IL-12p70 could not be detected in supernatants of DCs stimulated with LPS (data not shown). Nevertheless, mutual comparison (Figs. 5A and 5B) demonstrated that, in accordance with the results obtained with intact bacteria, the highest DC activation capacity was found for the LPS isolated from the BP2331-mutant strain, followed by those of the BP2328-mutant strain and the wild-type strain, whereas that of the BP2329-mutant strain was incapable of maturing DCs. Thus, the alterations in the LPS structure of the mutants differentially affect DC activation capacity.

Endotoxic activity of LPS and whole bacterial cells

To assess the consequences of the LPS mutations on the endotoxic activity of LPS, the potency of the purified LPS to stimulate the human macrophage cell line MM6 for IL-6 production was tested. As compared with wild-type LPS, purified LPS from the BP2331-mutant strain had a strongly increased potency to stimulate the macrophages (Fig. 6A). In contrast, LPS from the BP2329-mutant strain had a reduced potency to stimulate IL-6 production, whereas LPS from the BP2328 mutant was similarly active as wild-type LPS (Fig. 6A). Only at the two highest LPS concentrations tested, the latter LPS was more active than wild-type LPS was. Consistent with the data obtained with purified LPS, whole-cell suspensions of the BP2331 mutant showed, as compared to wild-type cells, a clearly increased potency to stimulate the macrophages (Fig. 6B). However, also the BP2328-mutant cells showed this effect (Fig. 6B), while BP2329-mutant cells had similar activity as the wild-type cells in spite of their less active purified LPS (Fig. 6A).

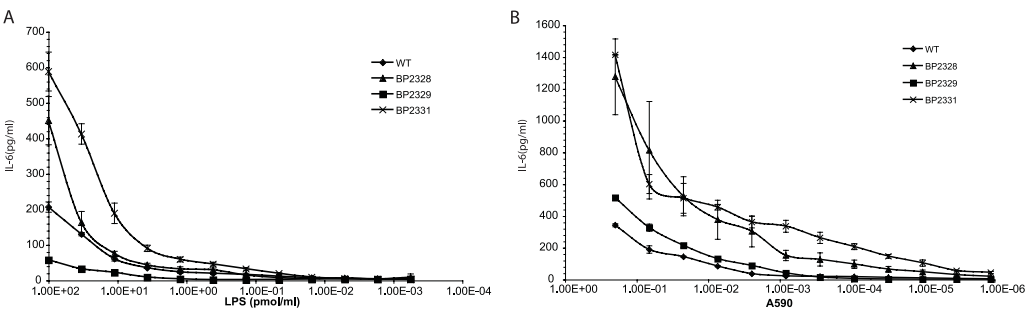

Fig. 6. IL-6 induction by purified *B. pertussis* LPS and whole bacterial cells. The production of IL-6 by the human macrophage cell line MM6 was stimulated with serial dilutions of stock solutions of purified LPS (A) or whole bacterial cells (B) from the wild-type *B. pertussis* strain (WT), or the BP2328-, BP2329-, and BP2331-mutant strains. IL-6 concentrations in the culture supernatants were quantified in an ELISA against human IL-6. The data represent the averages of three individual experiments.

Discussion

The goal of the present study was to identify new LPS glycosyltransferases in the *B. pertussis* genome. By using sequences of known LPS glycosyltransferases as leads, we were able to identify a four-gene operon. In a previous study, in which the genome sequence of the poultry pathogen *Bordetella avium* was compared to the genome sequences of other *Bordetellae*, an gene cluster homologous to the one here identified was described as being involved in LPS biosynthesis (Sebaihia *et al.*, 2006). However, no functional studies were reported which could confirm this assignment.

To study the role of this operon in *B. pertussis* LPS biosynthesis, we inactivated the putative glycosyltransferase genes by allelic exchange and compared the LPS profiles of the wild-type and mutant strains using Tricine-SDS-PAGE and ESI-MS. Unexpectedly, we found that the wild-type strain not only contained full-length *B. pertussis* LPS, but also harboured a full-length species substituted with an extra hexosamine moiety, which, as we showed, was directly attached to lipid A. Substitution of *B. pertussis* lipid A with hexosamine has previously not been observed and therefore represents a novel modification of *B. pertussis* lipid A.

The proposed truncated oligosaccharide structures for the BP2328- and BP2329- mutant strains are summarised in Fig. 7. The most complete core OS structure in the BP2328 mutant strain consisted of GalNA•Glc•$GlcN_2$•GlcA•Hep_2•*P*•Kdo attached to lipid A-OH, suggesting that the BP2328 mutant strain lacks the terminal trisaccharide and heptose residues. Since it has been demonstrated that addition of the trisaccharide is determined by the *wlb* locus (Allen and Maskell, 1996; Allen *et al.*, 1998b), the BP2328-encoded protein could function as a heptosyltransferase responsible for the attachment of the terminal heptose (Fig. 7. option 1). If this assumption is correct, it would implicate that the trisaccharide can only be added to the 6 position of the GlcN after the heptose has been added to the 4 position by the BP2328-encoded enzyme. Alternatively, because we identified here a novel modification of *B. pertussis* lipid A with hexosamine, it is also possible that one of the GlcN residues in the structure mentioned above is actually the novel hexosamine attached to lipid A. If this assumption is correct, it would implicate that the BP2328-mutant strain misses, besides the terminal trisaccharide and heptose, also a GlcN residue from the core OS and, thus, that the BP2328-encoded protein functions as a GlcN(1-4) to Glc transferase (Fig. 7, option 2). From the results obtained, it is impossible to discriminate between these two alternatives and further MS analysis will be required to determine the precise location of the HexN residue in question. Analysis of the BP2329-mutant LPS showed that this LPS was further truncated and that its most complete structure consisted of $GlcN_2$•GlcA•Hep_2•*P*•Kdo•lipid A-OH. Since this

structure misses the Glc to which the second GlcN of the core OS should be connected, one of the two GlcN residues indicated in the structure mentioned must represent the novel HexN residue attached to lipid A. Therefore, this composition suggests that the BP2329-encoded protein functions as a glucosyltransferase that attaches Glc to the first heptose subunit (Fig. 7). This would agree with the high homology of this gene product with glucose (β1-4) heptose transferases, such as *rfaK* and *lgtF/icsB*, which were used to identify the gene in the first place. The most complicated phenotype was observed in the case of the BP2331 mutant. Although the protein shows high sequence similarity to various LPS glycosyltransferases, full-length *B. pertussis* LPS was still present in the mutant strain. This observation suggests either that the BP2331 gene does not encode an active LPS glycosyltransferase or that the encoded enzyme shows redundancy. Consistent with this last option, we have identified a gene, i.e., BP3671 with GenBank Accession Number CAE43928, in the genome of *B. pertussis* which encodes for a protein that shows 69% identity to the BP2331-encoded protein. Albeit the LPS profiles of the wild-type and BP2331-mutant strain were more or less comparable, one striking observation was that the mutant LPS was more heterogenic. Although the exact reason for this phenomenon remains to be elucidated, one possible explanation could be that the BP2331 mutant somehow displays an increased non-stoichiometrical substitution of its LPS, possibly with hexosamine. Of note, besides the three glycosyltransferase homologs described above, the here identified gene cluster contains a fourth gene, i.e., BP2330, which encodes for a deacetylase. Modification of lipid A with amino sugars has

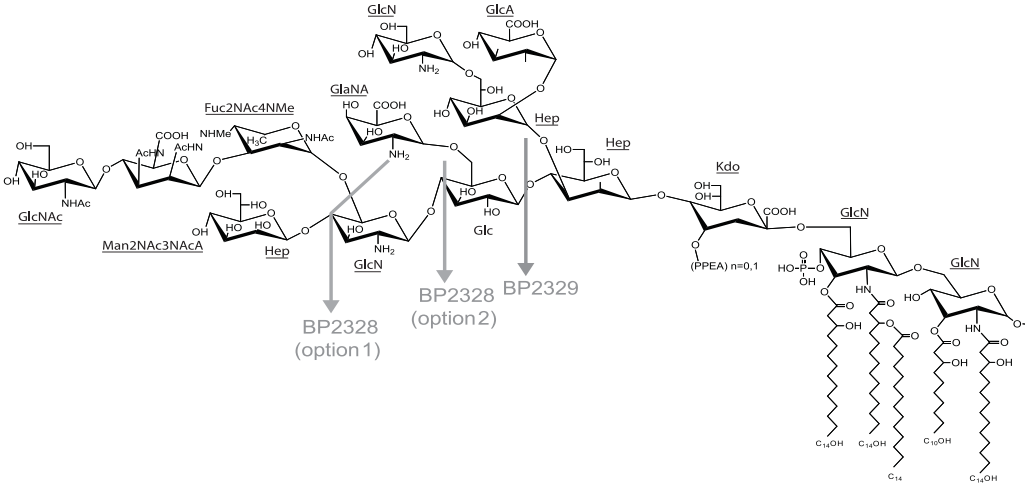

Fig. 7. Structure of *B. pertussis* LPS. Proposed truncated core OS structures of the BP2328- and BP2329-mutant strains are indicated by red arrows. Adapted from Caroff *et al*. (2000).

been described in various bacteria, e.g., substitution with 4-aminoarabinose in *E. coli* and *Salmonella* (Trent *et al.*, 2001b), and with galactosamine in *Francisella tularensis* (Phillips *et al.*, 2004). The aminoarabinose pathway has been studied in detail in *E. coli* and has been shown to involve the assembly of the sugar moiety on a separate undecaprenyl phosphate carrier prior to its transfer to lipid A (Trent *et al.*, 2001a). This pathway includes the ArnD deformylase required for freeing the amino group. Since it is conceivable that insertion of the kanamycin-resistance cassette in BP2331 has increased the expression of the downstream BP2330 gene, and one could speculate that the BP2330-encoded protein functions, by analogy, as the deacetylase responsible for releasing acetate from the amino group of hexosamine before it is attached to lipid A, it is tempting to speculate that an increased BP2330 expression may have led to an increased hexosamine modification of lipid A, and, consequently, an increased LPS heterogeneity in the BP2331-mutant cells. Further quantitative analysis of the presence of this modification, as well as the construction of mutants altered in the dedicated biosynthetic pathway, will be required to test this hypothesis.

After having addressed the structure of the LPS, purified LPS and whole bacterial cells were tested for their ability to induce maturation of DCs and to stimulate the production of pro-inflammatory cytokines by human macrophages. The results showed that, as compared to the wild-type strain, the BP2331-mutant strain displayed an increased capacity to induce DC maturation and pro-inflammatory cytokine production. Similar outcomes were obtained with purified LPS. In contrast, whole bacterial cells and purified LPS from the BP2328- and BP2329-mutant strains displayed a similar and decreased capacity to maturate DCs and stimulate macrophages, respectively. These results show that alterations in LPS core OS-composition differentially affect the biological properties of *B. pertussis* LPS. From the perspective of vaccine development, this is an interesting finding, since this may allow for the development of strains that more efficiently prime immune responses. Furthermore, mutants that display an increased LPS heterogeneity, such as the BP2331-mutant strain, may elicit a larger variety of anti-LPS antibodies, which, on itself, may positively influence vaccine efficacy.

References

Allen, A. G., Isobe, T., and Maskell, D. J. (1998a) Identification and cloning of *waaF* (*rfaF*) from *Bordetella pertussis* and use to generate mutants of *Bordetella* spp. with deep rough lipopolysaccharide. *J. Bacteriol.* **180:** 35-40.

Allen, A. G., Thomas, R. M., Cadisch, J. T., and Maskell, D. J. (1998b) Molecular and functional analysis of the lipopolysaccharide biosynthesis locus *wlb* from *Bordetella pertussis*, *Bordetella parapertussis* and *Bordetella bronchiseptica*. *Mol. Microbiol.* **29:** 27-38.

Allen, A., and Maskell, D. (1996) The identification, cloning and mutagenesis of a genetic locus required for lipopolysaccharide biosynthesis in *Bordetella pertussis*. *Mol. Microbiol.* **19:** 37-52.

Caroff, M., Brisson, J., Martin, A., and Karibian, D. (2000) Structure of the *Bordetella pertussis* 1414 endotoxin. *FEBS Lett.* **477:** 8-14.

Clementz, T., and Raetz, C. R. H. (1991) A gene coding for 3-deoxy-D-manno-octulosonic-acid transferase in *Escherichia coli*. Identification, mapping, cloning, and sequencing. *J. Biol. Chem.* **266:** 9687-9696.

Di Fabio, J. L., Caroff, M., Karibian, D., Richards, J. C., and Perry, M. B. (1992) Characterisation of the common antigenic lipopolysaccharide O-chains produced by *Bordetella bronchiseptica* and *Bordetella parapertussis*. *FEMS Microbiol. Lett.* **76:** 275-281.

Geurtsen, J., Steeghs, L., Hamstra, H-J., ten Hove, J., de Haan, A., Kuipers, B., Tommassen, J., and van der Ley, P. (2006) Expression of the lipopolysaccharide-modifying enzymes PagP and PagL modulates the endotoxic activity of *Bordetella pertussis*. *Infect. Immun.* **74:** 5574-5585.

Hanahan, D. (1983) Studies on transformation of *Escherichia coli* with plasmids. *J. Mol. Biol.* **166:** 557-580.

Holst, O. (2000) Deacylation of lipopolysaccharides and isolation of oligosaccharides phosphates. in *Methods in Molecular Biology, Bacterial Toxins: Methods and Protocols* (Holst, O., Ed.) pp 345-353, Humana Press, Totowa, NJ.

Heinrichs, D. E., Yethon, J. A., and Whitfield, C. (1998) Molecular basis for structural diversity in the core regions of the lipopolysaccharides of *Escherichia coli* and *Salmonella enterica*. *Mol. Microbiol.* **30:** 221-232.

Isobe, T., White, K. A., Allen, A. G., Peacock, M., Raetz, C. R. H., and Maskell, D. J. (1999) *Bordetella pertussis waaA* encodes a monofunctional 2-keto-3-deoxy-*D*-manno-octulosonic acid transferase that can complement an *Escherichia coli waaA* mutation. *J. Bacteriol.* **181:** 2648-2651.

Kasuga, B., Nakase, Y., Ukishima, K., and Takatsu, K. (1953) Studies on *Haemophilus pertussis*. *Kitasato Arch. Exp. Med.* **27:** 21-28.

Kurzai, O., Schmitt, C., Claus, H., Vogel, U, Frosch, M, and Kolb-Maurer, A. (2005) Carbohydrate composition of meningococcal lipopolysaccharide modulates the interaction of *Neisseria meningitidis* with human dendritic cells. *Cell. Microbiol.* **7**: 1319-1334.

Laemmli, U. K. (1970) Cleavage of structural proteins during the assembly of the head of bacteriophage T4. *Nature* **227:** 680-685.

Lesse, A. J., Campagnari, A. A., Bittner, W. E., and Apicella, M. A. (1990) Increased resolution of lipopolysaccharides and lipooligosaccharides utilizing tricine-sodium dodecyl sulfate-polyacrylamide gel electrophoresis. *J. Immunol. Methods* **126:** 109-117.

MacLachlan, P. R., Kadam, S. K., and Sanderson, K. E. (1991) Cloning, characterization, and DNA sequence of the *rfaLK* region for lipopolysaccharide synthesis in *Salmonella typhimurium* LT2. *J. Bacteriol.* **173**: 7151-7163.

O'Neill, L. A. J. (2006) How Toll-like receptors signal: what we know and what we don't know. *Curr. Opin. Immunol.* **18:** 3-9.**Pålsson-McDermott, E. M., and O'Neill, L. A. J.** (2004) Signal transduction by the lipopolysaccharide receptor, Toll-like receptor-4. *Immunology* **113:** 153-162.

Peppler, M. S. (1984) Two physically and serologically distinct lipopolysaccharide profiles in strains of *Bordetella pertussis* and their phenotype variants. *Infect. Immun.* **43:** 224-232.

Phillips, N. J., Schilling, B., McLendon, M. K., Apicella, M. A., and Gibson, B. W. (2004) Novel modification of lipid A of *Francisella tularensis*. *Infect. Immun.* **72:** 5340-5348.

Plüddeman, A., Mukhopadhyay, S., and Gordon, S. (2006) The interaction of macrophage receptors with bacterial ligands**.** *Exp. Rev. Mol. Med.* **8**: 1-25.

Raetz, C. R. H., and Whitfield, C. (2002) Lipopolysaccharide endotoxins. *Annu. Rev. Biochem.* **71:** 635-700.

Sallusto, F., and Lanzavecchia, A. (1994) Efficient presentation of soluble antigen by cultured human dendritic cells is maintained by granulocyte/macrophage colony-stimulating factor plus interleukin 4 and downregulated by tumor necrosis factor α. *J. Exp. Med*. **179**: 1109-1118.

Schnaitman, C. A., and Klena, J. D. (1993) Genetics of lipopolysaccharide biosynthesis in enteric bacteria. *Microbiol. Rev.* **57:** 655-682.

Sisti, F., Fernández, J., Rodríguez, M. E., Lagares, A., Guiso, N., and Hozbor, D. F. (2002) In vitro and in vivo characterization of a *Bordetella bronchiseptica* mutant strain with a deep rough lipopolysaccharide structure. *Infect. Immun.* **70:** 1791-1798.

Steeghs, L., van Vliet, S. J., Uronen-Hansson, H., van Mourik, A., Engering, A., Sanchez-Hernandez, M., Klein, N., Callard, R., van Putten, J. P. M., van der Ley, P., van Kooyk, Y., and van de Winkel, J. G. J. (2006) *Neisseria meningitidis* expressing *lgtB* lipopolysaccharide targets DC-SIGN and modulates dendritic cell function. *Cell. Microbiol.* **8:** 316-325.

Stibitz, S. (1994) Use of conditionally counterselectable suicide vectors for allelic exchange. *Methods Enzymol.* **235:** 458-465.

Takada H, and Kotani S. (1989) Structural requirements of lipid A for endotoxicity and other biological activities. *Crit. Rev. Microbiol.* **16:** 477-523.

Thalen, M., van den IJssel, J., Jiskoot, W., Zomer, B., Roholl, P., de Gooijer, C., Beuvery, C., and Trampen, J. (1999) Rational medium design for *Bordetella pertussis*: basic metabolism. *J. Biotechnol.* **75:** 147-159.

Trent, M. S., Ribeiro, A. A., Doerrler, W. T., Lin, S., Cotter, R. J., and Raetz, C. R. H. (2001a) Accumulation of a polyisoprene-linked amino sugar in polymyxin-resistant *Salmonella typhimurium* and *Escherichia coli*: structural characterization and transfer to lipid A in the periplasm. *J. Biol. Chem.* **276:** 43132-43144.

Trent, M. S., Ribeiro, A. A., Lin, S., Cotter, R. J., and Raetz, C. R. H. (2001b) An inner membrane enzyme in *Salmonella* and *Escherichia coli* that transfers 4-amino-4-deoxy-L-arabinose to lipid A: induction on polymyxin-resistant mutants and role of a novel lipid-linked donor. *J. Biol. Chem.* **276:** 43122-43131.

Tsai, C. M., and Frasch, C. E. (1982) A sensitive silver stain for detecting lipopolysaccharides in polyacrylamide gels. *Anal. Biochem.* **119:** 115-119.

Uronen-Hansson, H., Steeghs, L., Allen, J., Dixon, G.L.J., Osman, M., van der Ley, P., Wong, S.Y.C., Callard, R., and Klein, N. (2004) Human dendritic cell activation by *Neisseria meningitidis*: phagocytosis depends on expression of lipooligosaccharide (LOS) by the bacteria and is required for optimal cytokine production. *Cell. Microbiol.* **6**: 625-637.

van Amersfoort, E. S., Van Berkel, T. J., and Kuiper, J. (2003) Receptors, mediators, and mechanisms involved in bacterial sepsis and septic shock. *Clin. Microbiol. Rev.* **16:** 379-414.

Viera, J. and Messing, J. (1982). The pUC plasmids, an M13mp7-derived system for insertion mutagenesis and sequencing with synthetic universal primers. *Gene* **19**: 259-268.

Westphal, O., and Jann, J. K. (1965) Bacterial lipopolysaccharides, extraction with phenol-water and further applications of the procedure. *Methods Carbohydr. Chem.* **5:** 83-91.

Ziegler-Heitbrock, H. W. L., Thiel, E., Futterer, A., Herzog, V., Wirtz, A., and Riethmüller, G. (1988) Establishment of a human cell line (Mono Mac 6) with characteristics of mature monocytes. *Int. J. Cancer* **41:** 456-461.